Surfactant adsorption density calculation from Fourier transform infrared external reflection spectroscopy (FTIR/ERS)

Keqing Fa[a] and Jan D. Miller
Department of Metallurgical Engineering, University of Utah, Salt Lake City, Utah 84112

(Received 7 July 2003; accepted 30 September 2003)

An equation to calculate surfactant adsorption density from Fourier transform infrared external reflection spectra was established. The derivation and limitation of this equation are discussed in detail. The validation of the FTIR/ERS adsorption density equation was experimentally verified from the analysis of Langmuir–Blodgett films of stearic acid with and without calcium ions in the subphase at the air–water interface and at fluorite surface. In this way the properties of Langmuir–Blodgett films at the air–water interface are further characterized using FTIR/ERS. © *2003 American Institute of Physics.* [DOI: 10.1063/1.1628224]

I. INTRODUCTION

Because of easy manipulation and definition of the thin film properties, and the ability to modify the film through variation in subphase solution chemistry, the Langmuir–Blodgett method has been used with good success for the studies in chemical, biomedical, and pharmaceutical fields.[1] The surfactants, which can be compressed at the air–water interface, are amphiphilic molecules. Their polar heads are in the water subphase while their hydrocarbon chains are directed toward the air phase. The structure and stability of the Langmuir–Blodgett films at the air–water interface are strongly affected by many factors such as hydrocarbon chain length, molecule solubility, temperature, solution pH and the present of cations and organic–polymer molecules in the subphase.[2–11] It has been noted that the addition of divalent cations such as Pb^{2+}, Cu^{2+}, Zn^{2+}, Ca^{2+}, and Fe^{2+} and organic–polymer molecules in the subphase can enhance not only the stability of amphiphilic molecules at air–water interface but subsequently their transfer and deposition at a rigid surface.[2–8,11–17] The explicit change of adsorption isotherms with the addition of divalent cations is indicative of solution chemistry effects on Langmuir–Blodgett film phases. The interaction between cations and surfactant molecules at the air–water interface has been discussed using the double layer theory.[6]

The influence of cations and polymer–organic molecules on Langmuir–Blodgett films and the characteristics of the Langmuir–Blodgett films have been studied by many modern scientific tools including transmission electron microscopy (TEM),[5] atomic force microscopy (AFM) imaging,[10] ellipsometry,[18] surface potential, light scattering, x-ray diffraction,[5] FTIR and fluorescence microscopy.[9] Among them, FTIR/ERS is a very promising tool because it is nondestructive, sensitive to chemical states, and *in situ* monitoring of Langmuir–Blodgett films. For example, the orientation angle of transition dipole moment of surfactant molecules can be measured using linear dichroism theory.[19,20] This angle indicates the surfactant tilt angle with respect to the surface normal. Since first introducing ERS sampling at air–water interface,[21–23] Dluhy and co-worker have reported the two-dimensional (2D) infrared (IR) correlation analysis of phase transition in Langmuir films at air–water interfaces.[24–27] The 2D IR correlation analysis enhances the resolution of overlapped peaks. Thus this method has been successful to the phase analysis of films. C–H stretching peaks are sensitive to the molecular environmental change. The molecular ordering information can consequently be obtained by monitoring vibration frequency shifting of C–H stretching.[28,29]

Recently, Takeshi Hasegawa *et al.* have attempted to make quantitative measurements using FTIR/ERS[30] at the air–film–solid crystal substrate such as silicon, germanium. These researchers found that the experimentally measured absorbance of thin films on these substrates were different from the theoretically calculated values. The main reason for this discrepancy was thought to be the high reflectivity of the infrared light from the bottom surface of the experimental substrate, which turned the experimental setup into a complex optical system rather than the intended three-phase model. Mielczarski *et al.* used the calculated absorbance from simulation as a reference to estimate the number of adsorbed layers.[31,32] However, to our knowledge, there are no equations or formulas which have been developed to calculate the adsorption density (mol/m^2) from ERS spectra. Adsorption density is a very important variable because in some systems it could reveal the phases and adsorption mechanism of the film at surfaces. For the first time in this paper, an ERS adsorption density equation has been established. As the first step of research, the adsorption densities of Langmuir–Blodgett films at the air–water interface have been calculated from FTIR/ERS spectra for stearic acid with and without calcium ions in the subphase. The ultimate goal of this research is to develop an ERS equation to calculate the surfactant adsorption density for self-assembled film at solid state substrates. However, the quantitative analysis method presented in the current paper is derived and verified based on Langmuir–Blodgett films because the Langmuir–

[a]Author to whom correspondence should be addressed. Telephone: (801) 581 6814; Fax: (801) 581 4937; Electronic mail: kfa@mines.utah.edu

Blodgett film can be well controlled and the surfactant adsorption density can also be calculated from the Langmuir–Blodgett film isotherm.

II. EXPERIMENT

A. Materials and equipment

Stearic acid (+98% pure) obtained from Sigma Chemical was used without further purification. Chloroform (spectrophotometric grade), calcium chloride, and sodium hydroxide were used as received from Mallinckrodt. Carbon tetrachloride was also used as received from Aldrich Chemical Co., Inc. High purity Milli-Q water (+18 MΩ cm) was used throughout the experiments. Circular transmission windows of fluorite were purchased from Harrick Scientific Corporation.

The 800×200 mm^2 Langmuir–Blodgett trough was manufactured by NIMA, England, Model 2001. FTIR experiments were conducted with a dry-air and liquid N_2 purged Bio-Rad Digilab Division FTS-6000 FTIR spectrometer equipped with a liquid-nitrogen-cooled wide-band mercury cadmium telluride (MCT) detector. An external reflection accessory accompanied with a miniature trough with an effective area 8.2×2.18 cm was purchased from Spec Inc.

B. Langmuir–Blodgett films

The isotherms of stearic acid films with and without calcium ions in the subphase at the air–water interface were obtained using the Langmuir–Blodgett trough. The stearic acid chloroform solution with the concentration at 1 mg/ml was spread drop by drop on the deionized (DI) water surface (80 μl for without calcium ions and 120 μl for with calcium ions). The chloroform was allowed to evaporate for 30 min before compression. The compression velocity was set at 30 cm^2/min. Stearic acid Langmuir–Blodgett films without calcium ions in the subphase were obtained when the subphase was pure water with a neutral pH. The Langmuir–Blodgett films with calcium ions in the subphase were compressed when the subphase contained 2×10^{-3} M $CaCl_2$ and had a pH of 9.0–9.5.

A fluorite IRE substrate was cleaned with methanol and acetone, and then plasma treatment for five minutes on each side. Before spreading of stearic acid on the water subphase, the IRE substrate was first dipped into the subphase. The three-phase system—air, LB film, and fluorite substrate was prepared on one side of the fluorite crystal. In order to accomplish this, two identical calcium fluoride crystals were used in the film transfer. The LB film deposition was realized by a back-to-back deposition technique, in which the two identical crystals were bonded together with only one side of each crystal exposed to surfactant molecules. The substrates were withdrawn at a speed of 3 mm/min with the surface pressure held at the desired point. The transferred film quality was evaluated by the transfer ratio (TR), which is the area decrease on the water surface between two movable bars over the calculated solid crystal area which is exposed to the stearic acid molecules. In all experiments, if the TR was outside the range of 90%–110%, the experiments were repeated.

C. Infrared analysis

One miniature trough with an effective spreading area of about 18 cm^2 or the fluorite crystal was attached to the angle adjustable external reflection accessory. All the external reflection spectra were recorded at an angle of incidence of 20°. The details of why this angle was chosen will be discussed during derivation of the FTIR/ERS adsorption density equation. Unpolarized radiation was used to increase the signal to noise ratio, S/N. The absorbance was defined as $-\log(R/R_o)$, where R and R_o are the reflectivities of the system with and without the surfactant, respectively. Both sample and reference spectra were averaged over the same numbers of scans, 1024. All spectra were obtained at a resolution of 8 cm^{-1}.

For the analysis at air–water interface, the chloroform solution of stearic acid with a concentration at 0.06 mg/ml was prepared with the help of a microgram scale balance. The chloroform solution was deployed using a 50 μl syringe by allowing the drops to "touch" the water surface, i.e., the drops were as close as possible to the water surface. The droplets were distributed over the entire trough area with an effective parking area of about 0.45 nm^2 per molecule, and the solvent was allowed to evaporate for 20 min before starting the infrared measurements. Then the monolayer was compressed discontinuously and slowly to desired levels of compression. By knowing the total amount of molecules spread at the air–water interface and measuring the trough area with a calibrated scale, the area per molecule values (degree of compression) were calculated.

For the analysis at the fluorite surface, a strong absorbing material was placed under the fluorite crystal to eliminate the reflection from the metal surface of external reflection accessory. The bottom surface of the fluorite crystal was roughened to remove the reflection of IR light from the bottom surface.

Traditional transmission spectra at various concentrations were also recorded to measure the absorptivity of stearic acid.

D. Spectral simulation

It is useful and important to compare the experimental measurements with spectral simulations. Many researchers[33–35] have done such simulations based on Hansen's exact equations published in the 1960s or using the Fresnel equations. The mathematical algorithm developed in this research follows Hansen's exact equations.[36–39] A three-layer model with parallel phase boundaries consisting of an isotropic and semi-infinite incidence medium, an isotropic adsorbate film of thickness d, and an isotropic and semi-infinite substrate was used. Simulation was achieved in computer language C++. It is worthwhile to point out that Langmuir–Blodgett films are uniaxially anisotropic films instead of isotropic films. Thus it is expect that the calculated absorbances are slightly different from the measured results. However, the results from simulation are instructive by carefully selecting optical constants for the three-phase system.

An example of the simulation results is shown in Fig. 1. The refractive indices of the incident phase (air) and the

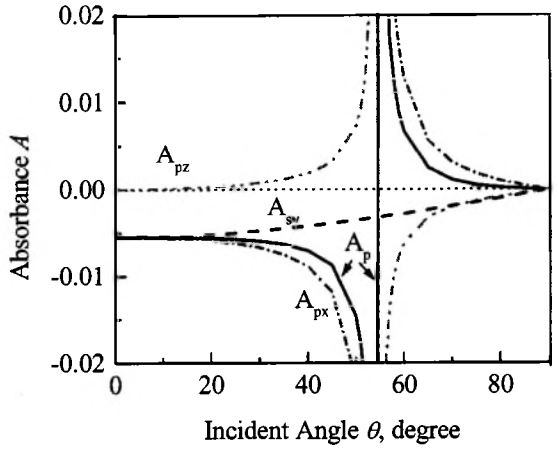

FIG. 1. FTIR/ERS spectral simulation for a 2.8 nm layer of stearic acid at air–water interface at 2920 cm^{-1}. Solid line: *p*-polarization; Dashed line: *s*-polarization. Three phase layer system: air ($n_1=1$, $k_1=0$); hypothetical Langmuir–Blodgett film of stearic acid ($n_2=1.48$, $k_2=0.20$); water ($n_3=1.40$, $k_3=0$).

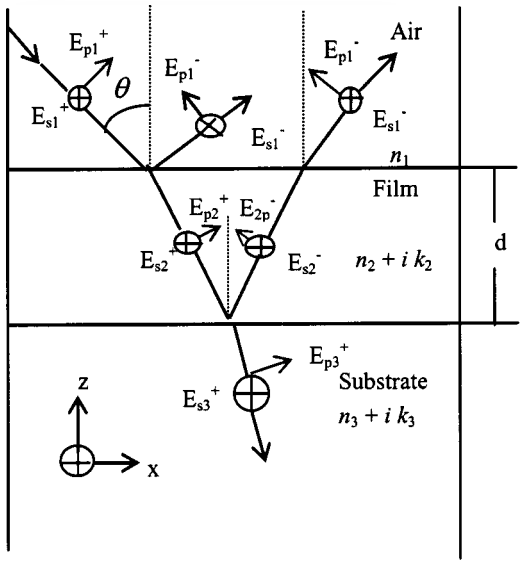

FIG. 2. Schematic of electric field components of IR radiation passing through three phase medium.

substrate (water) were selected as $n_{air}=1$, $n_{water}=1.40$, respectively, and the substrate phases were assumed to be nonabsorbent ($k=0$) at 2920 cm^{-1} (for water, $k=0.0082$ at this wave number, which is small enough to be neglected.).[40]

III. FTIR/ERS ADSORPTION DENSITY EQUATION

The reflection spectra of films at a surface are, in general, different from the corresponding transmission spectra of the same film without support. The differences originate from orientation, surface perturbation, optical effects including refractive index dispersion, and the anisotropic and periodic nature in three directions of the electromagnetic field at the surface.[41–44] The intensity, position, sign, and shape of spectra recorded using FTIR/ERS show a strong dependency on incident angle (Fig. 1), substrate optical properties, IR radiation polarization, and surfactant orientation at the surface. Therefore, distinguishing the changes observed in the reflection spectra, which are caused by optical effects from those changes due to surfactant adsorption density and surfactant structure is crucial for quantitative measurements and must be done first.

A. Incident angle limitation

Figure 2 shows a schematic of infrared radiation passing through a three-layer system. *E* represents the electric field of the radiation. The subscripts *s* and *p* indicate perpendicular and parallel components of the light, respectively. Numbers 1, 2, and 3 distinguish the phases. Superscripts + and − mean the components diffracted and reflected, respectively. It is well known that the Beer–Lambert law provides a quantitative measurement of molecule concentration from the optical spectra. The Beer–Lambert law is:

$$A=\epsilon\cdot c\cdot l=\frac{\alpha}{\ln(10)}\cdot l=\frac{4\pi}{\ln(10)}\cdot\frac{kl}{\lambda}, \tag{1}$$

where *A* is the integrated absorbance (cm^{-1}), ϵ is the molecule absorptivity (L/cm^2mol), *c* is the concentration (mol/L), and *l* (cm) is the optical path length, α is the absorption coefficient, *k* is the extinction coefficient, λ is the wavelength in vacuum (cm).

In transmission experiments, the Beer–Lambert law is valid because the absorption band only results from the molecular absorption of IR radiation, which has the exact energy to excite a molecule along the radiation path from a ground state to high-energy state. However, Fig. 1 clearly shows that the intensity of ERS spectra is determined not only by the adsorbed surfactant but also by the incident angles. It can be seen that the absorbance of *s*-polarization is negative for all-incident angles and decreases monotonically with an increase of the incident angle. But the absorbance of *p*-polarization light changes from negative for low incident angles to positive for high incident angles. This change is very sharp when the incident angle is near the Brewster angle (θ_B), which is 54.46° for the film–water interface ($n=1.40$ at $\lambda=2920$ cm^{-1} for water). The *p*-polarization can be further resolved into two components: Parallel absorbance A_{px} and perpendicular absorbance A_{pz}.[31,41] For $\theta<\theta_B$, A_{pz} is positive and A_{px} is negative. The reverse applies for $\theta>\theta_B$. When using unpolarized light and an incident angle larger than θ_B, it is expected that there is absorbance cancellation between *s*-polarization and *p*-polarization in the IR spectra due to the opposite signs of absorbance. Thus the incident angle should not be selected in this range for quantitative measurements.

If approximate equations are used, the theoretical absorbance for the three components A_{sy}, A_{px}, and A_{pz} can be calculated as follows:[35,39]

$$A_{sy}=-\frac{16\pi}{\ln 10}\left[\frac{\cos\theta}{n_3^2-1}\right]\frac{n_{2y}k_{2y}d_2}{\lambda}, \tag{2}$$

$$A_{px}=-\frac{16\pi}{\ln 10}\left[\frac{\cos\theta}{\xi_3^2/n_3^4-1}\right]\left[-\frac{\xi_3^2}{n_3^4}\right]\frac{n_{2x}k_{2x}d_2}{\lambda}, \tag{3}$$

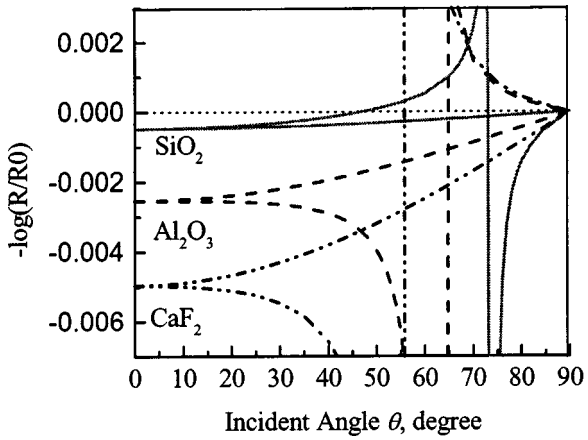

FIG. 3. FTIR/IR spectral simulation for a 2.8 nm layer of stearic acid at fluorite, sapphire and silicon substrates at 2920 cm^{-1}. First Phase: $n_1=1$, $k_1=0$; Second Phase: $n_2=1.576$, $k_2=0.246$; Third Phase: fluorite $n_3=1.43$, sapphire $n_3=1.74$, silicon $n_3=3.4$; $k_3=0$.

$$A_{pz}=-\frac{16\pi}{\ln 10}\left[\frac{\cos\theta}{\xi_3^2/n_3^4-1}\right]\left[-\frac{\sin^2\theta}{(n_{2z}^2+k_{2z}^2)^2}\right]\frac{n_{2z}k_{2z}d_2}{\lambda}, \tag{4}$$

where $\xi_3=(n_3^2-n_1\sin^2\theta)^{1/2}$, λ is the wavelength in a vacuum, and n_3 should be complex, but Eqs. (2)–(4) can only be used since k_3 is zero. Note that n_{2i} and k_{2i} ($i=x$, y, and z) are the components of refractive indices and the extinction coefficients for the Langmuir–Blodgett film, respectively; d_2 is the thickness of the Langmuir–Blodgett film and θ is the incident angle for the system.

It is possible to find or measure the film optical constants (k_2 and n_2) and the substrate optical constants (n_3 and k_3). But it is not so easy to get the exact values of d_2, k_{2x}, k_{2y}, and k_{2z} for uniaxial films. Thus Eqs. (2)–(4) could not be used directly to calculate the molecular adsorption density from ERS spectra. In this regard, it is necessary to find a new equation based on Eqs. (2)–(4). Careful evaluation of the simulation results shown in Fig. 1 provides a very interesting suggestion. In the lower incident angle range, say θ from 0° to 20°, the absorbances of surfactant at the water surface, A_{sy} and A_{px} are very close and $A_{pz}\approx 0$ due to the factor $\sin^2\theta/(n_{2z}^2+k_{2z}^2)^2$. This leads to a simplification of Eq. (3). Because the value of $n_1\sin^2\theta=1.0\times\sin^2 20^\circ\approx 0.095$ is much less than n_3 (for example, water $n_3=1.40$ at ~2920 cm^{-1}), $\xi=n_3$ and $\xi^2/n_3^4\approx 1/n_3^2$, and $[\cos\theta/(\xi_3^2/n_3^4-1)][-\xi_3^2/n_3^4]$ can be simplified to $[\cos\theta/(n_3^2-1)]$, showing that under these circumstances Eqs. (2) and (3) are equivalent and thus $A_{sy}\cong A_{px}$. The equality of A_{sy} to A_{px} and the fact that $A_{pz}\approx 0$ are very important conditions in the derivation of ERS adsorption density equation, which is presented later. The selection of small incident angles thus makes the quantitative analysis insensitive to the variation of incident angles.

Figure 3 shows the expected absorbance of the same fatty acid film at the surface of three mineral crystals: fluorite (CaF_2, refractive index $n_3=1.43$), sapphire (Al_2O_3, refractive index $n_3=1.74$) and silicon (Si, refractive index $n_3=3.4$). It is evident that in each case the absorbances of *s*-polarized and *p*-polarized light are very close when the incident angle is smaller than 20 degree.

B. Influence of substrate

Hansen and other researchers have calculated the mean-square electric field (MSEF) at two phase and three phase interfaces.[36,37,41,42] For both internal reflection and external reflection systems, the electromagnetic field components along the three directions x, y, and z of the surface are anisotropic, which indicates that the spectral absorbance may vary with the change of substrate optical properties. Figure 3 shows some simulation results of how absorbance varies with the substrate indices. Assuming the adsorbed species with the exact same optical properties adsorbing on different substrates, the absorbance on the higher refractive index substrate is always smaller than that on the lower index substrate. When the incident angle is smaller than 20 degrees, A_{sy} and A_{px} are proportional to $1/(n_3^2-1)$. If the substrate is sapphire with refractive index $n_3=1.74$ and $n_3^2-1\approx 2.0$, it is expected that the measured absorbance of the same stearic acid film adsorbed at the sapphire surface will be half of that at the fluorite surface ($1.43^2-1\approx 1$), as shown in Fig. 3.

Based on the discussion above, in order to calculate the absorbance from ERS spectra, it is proposed that the measured absorbance be multiplied by $(n_3^2-1)/\cos\theta$. Multiplication converts the absorbance measured from ERS spectra into an absorbance similar to that from transmission spectra, only dependent on surfactant absorptivity, optical length, and surfactant concentration.

This paper presents FTIR/ERS experimental data collected from the air–water interface. The air–water interface instead of solid substrates such as sapphire or silicon was first chosen because in the case of solid substrate, the reflectance from the bottom surface of the crystal is difficult to eliminate completely, which results in the so-called higher order output of light.[30,45,46] The air–Langmuir–Blodgett film–water system is an ideal three-phase setup because the water subphase with a depth at 1 cm was used in present experiments. There is no significant reflectance from the bottom surface. In the CH vibration region used for quantitative analysis, the k value of water is very small. Nevertheless, its influence on the spectra has been investigated.[47] It has been found the effect of k of water was negligible. It is intended that the results will be published soon.[48]

C. Surfactant orientation at surfaces

The simulation assumes isotropic films at low absorbing surfaces. Intuitively, surfactant orientation at the surface should have an effect on the FTIR/ERS spectra. Langmuir–Blodgett films are not isotropic but uniaxial. Many studies have reported measurements of the aliphatic chain tilt angle of the surfactant molecule with respect to the surface normal. Jang and Miller reported that the angle between the molecular axis and the surface normal for stearic acid Langmuir–Blodgett films transferred at a fluorite surface is in the range of 9°–14°.[49] These measurements were conducted using FTIR/IRS. This means that the transition dipole moment of

the CH_2 group is almost parallel to the surface. The uniaxial Langmuir–Blodgett film has three different components (k_{2x}, k_{2y}, and k_{2z}) of the k_2 value, which are different from the k_2 values for isotropic films. The relationship between k_2 and k_{2i} ($i=x$, y, and z) can be simply treated as follows:[30,50–53]

$$k_{2x}=k_{2y}=\tfrac{3}{2}k_2\sin^2\phi, \tag{5}$$

$$k_{2z}=3k_2\cos^2\phi, \tag{6}$$

where ϕ is the angle between the transition moment and the molecule director. For the Langmuir–Blodgett film of stearic acid, if the molecule chain tilt angle is 10°–15°, ϕ is about 75°–80°. Thus k_{2z} is almost 0.0.

D. Derivation of the adsorption density equation

In the case of external reflection, the optical path length, l, is defined as follows:

$$l=2\cdot d/\cos\theta_f, \tag{7}$$

where d is the thickness of the film and θ_f is refractive angle in phase 2.

For unpolarized light, $A_{sy}\approx A_{px}$ and $A_{pz}\approx 0$, then substitute Eqs. (5) and (6) into Eqs. (2) and (3), the following relationship can be formed:

$$A^{\text{trans}}=A_{sy}^{\text{trans}}+A_{px}^{\text{trans}}=-\frac{n_3^2-1}{3n_{2xy}\cos\theta\cos\theta_f\sin^2\phi}\mathrm{A_{ERS}}. \tag{8}$$

Where A^{trans} stands for transmissionlike absorbance, $\mathrm{A_{ERS}}$ is the absorbance measured from the ERS spectra, $n_{2y}=n_{2x}=n_{2xy}$ is the index of refraction of films in xy plane.

After substitution of Eqs. (7) and (8) into Eq. (1), the following expression is formed:

$$\begin{aligned}-\frac{(n_3^2-1)}{3n_{2xy}\cos\theta\cos\theta_f\sin^2\phi}A_{\text{ERS}}&=\epsilon\cdot c\cdot 2\cdot d/\cos\theta_f\\&=2\cdot\epsilon\cdot(c\cdot d)/\cos\theta_f.\end{aligned} \tag{9}$$

Rewriting Eq. (9) and taking $c\cdot d$ as the adsorption density (Γ) at the surface

$$\Gamma=c\cdot d=-\frac{(n_3^2-1)A_{\text{RES}}}{6n_{2xy}\epsilon}\cdot\frac{1}{\cos\theta\sin^2\phi}. \tag{10}$$

Then making the units consistent, Eq. (10) becomes

$$\begin{aligned}\Gamma&=-\frac{10\cdot(n_3^2-1)\mathrm{A_{ERS}}}{6n_{2xy}\cdot\epsilon}\cdot\frac{1}{\cos\theta\sin\phi}\\&=-\frac{5(n_3^2-1)}{3n_{2xy}\epsilon}\cdot\frac{1}{\cos\theta\sin^2\phi}\cdot\mathrm{A_{ERS}},\end{aligned} \tag{11}$$

where the units are $\Gamma(\text{mol/m}^2)$, $A_{\text{ERS}}\,(\text{cm}^{-1})$, $\epsilon(\text{L/cm}^2\,\text{mol})$.

Equation (11) is the ERS adsorption density equation for one reflection at low angles of incidence. If the experimental setup is designed for multiple reflections (N reflections), A_{ERS} should be divided by N. The values of n_3 and n_{2xy} as well as ϵ can be found from the literature or measured, and θ is known. Also ϕ can be measured by dichroic method. Thus Eq. (11) allows for the calculation of adsorption density without knowing the film thickness and the three components of optical absorption coefficients. This is the advantage of Eq. (11) over Eqs. (2)–(4) and similar equations reported in Ref. 19.

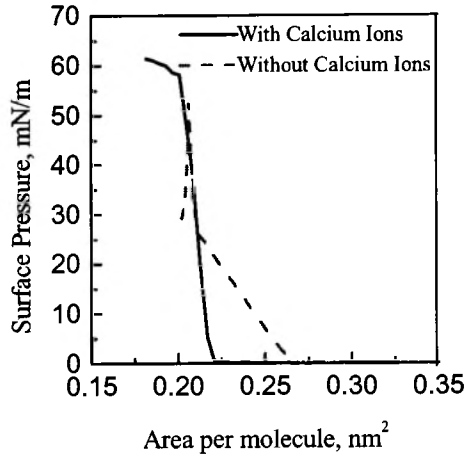

FIG. 4. Isotherms of stearic acid with and without calcium ions in the subphase.

IV. RESULTS AND DISCUSSION

A. Surface pressure-area isotherm for stearic acid with and without calcium ions in the subphase

Figure 4 shows the surface pressure-specific area (π-A) isotherms for stearic acid with and without calcium ions in the subphase at the air–water interface. These isotherms were found to be in good agreement with the isotherms reported in the literature.[6,53,54] Immediately it is clear that the stearic acid isotherm without calcium ions in the subphase exhibits a number of sharply separated regions of different compressibility. It is well known that the isotropic liquid and crystalline surface phases of stearic acid are not very stable at room temperature. This character of stearic acid prevents very good transfer of solid and liquid films at higher surface pressure to form multilayers. It is worthy to note that in the stearic acid isotherm, the liquid phase region is very narrow and quickly transforms to the solid state as the pressure is increased. The liquid phase begins at a pressure which corresponds to a surface area from 0.24 to 0.26 nm^2 per molecule.

The isotherm of stearic acid with calcium ions in the subphase is quite different from that of stearic acid without calcium ions. The main difference is that the liquid region is greatly reduced to the so-called condensed phase. The effect of the cation ions on the isotherms is complex and several theories have been proposed.[6] This change in the isotherm indicates that the film properties are also greatly altered. The condensed phase is very good for transfer and the creation of multilayer solid films.

B. Molar absorptivity by transmission experiments

To use Eq. (11), the ERS adsorption density equation, molar absorptivity must be determined *a priori*. The molar

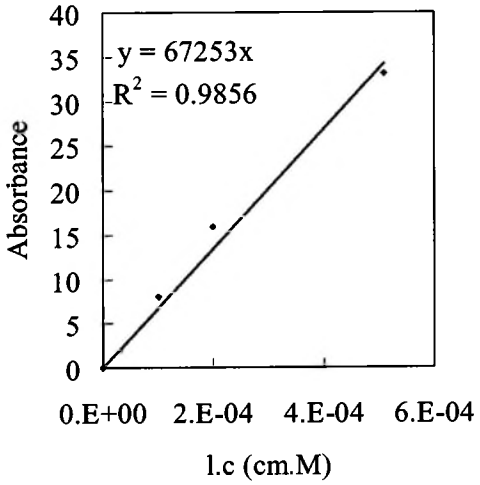

FIG. 5. Absorptivity of stearic acid.

absorptivity, ϵ, is measured by transmission using the Beer–Lambert law. Figure 5 shows the change in the integrated absorbance for the CH stretching region (2800–3050 cm^{-1}) with respect to the product of path length and stearic acid concentration in carbon tetrachloride ($l \cdot c$). The slope of the straight line was accepted as the molar absorptivity for stearic acid, ϵ=67 253 L/cm^2 mole, which is in excellent agreement with the literature, (ϵ=67 600 L/cm^2 mole).[55] Here we assume that the stearic acid film with and without calcium ions in the subphase has the same absorptivity.

C. Wave number of CH_2 stretching

It is known that the wave number of the CH_2 band is sensitive to the conformation of the molecule. Figure 6 shows the CH_2 vibrational spectra of stearic acid without calcium ions in the subphase collected at various area per molecule values. It is evident that the peaks shift to lower wave numbers once the films are compressed from a high area per molecule to a low area per molecule. The value of the small surface areas is indicative of the mainly all-trans conformation of the alkyl chain with few gauche conformers. On the other hand the higher wave numbers for surface areas larger than 0.28 nm^2 $molecule^{-1}$ indicate the inclusion of gauche conformers. The shift of the wave number is estimated to be about 1 cm^{-1}. Figure 6 shows that the molecules changed from a random state to a well-ordered conformation once the films were compressed properly.

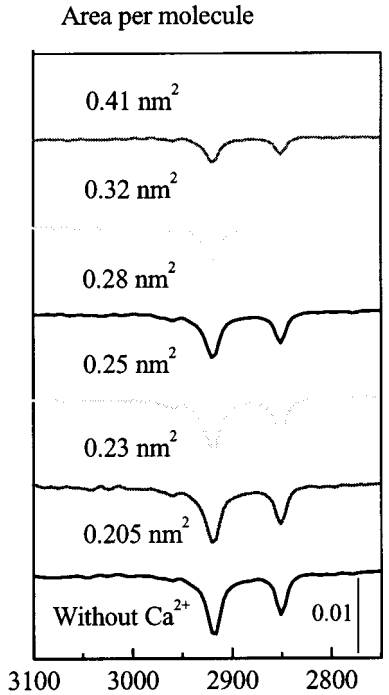

FIG. 6. External reflection spectra for the CH_2 vibration of a stearic acid monolayer without calcium ions in the subphase at air–water interface at various area per molecule values.

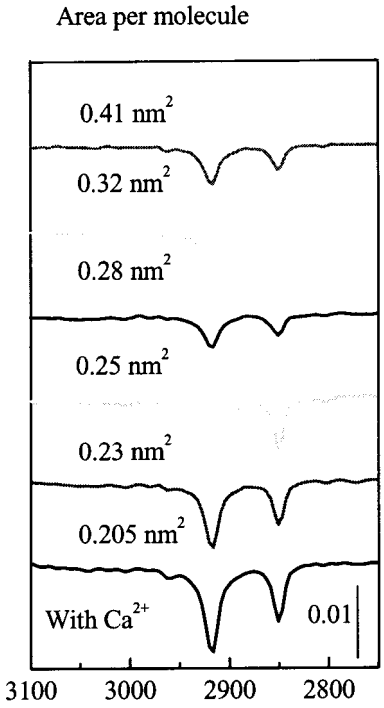

FIG. 7. External reflection spectra for the CH_2 vibration of a stearic acid monolayer with calcium ions in the subphase at air–water interface at various area per molecule values.

Spectra shown in Fig. 7 are the CH_2 vibrational bands of stearic acid films with calcium ions in the subphase at various area per molecule values. It is evident that the wave numbers of these peaks are smaller than those for the stearic acid Langmuir–Blodgett films, which means that the molecules are more in the all-trans conformation. Also the results show that the wave numbers do not shift upon compression. This further confirms that the molecules are well ordered at the air–water interface even at the very beginning of compression.

D. Adsorption density of stearic acid at air–water interface

Table I presents the calculated area per molecule values from both the Langmuir–Blodgett experiment and from the ERS adsorption density equation. The refractive index of water at 2920 cm^{-1} was reported as 1.40.[40,54] The refractive index of stearic acid Langmuir–Blodgett films in the xy plane was set to 1.48.[30,51] The angle ϕ was taken as 75°

TABLE I. Comparison of adsorption densities calculated from Langmuir–Blodgett experiments with that predicted from ERS equation for streric acid film at air–water interface.

	Without calcium ions in the subphase		With calcium ions in the subphase	
Experiment Langmuir–Blodgett area per molecule, nm^2	Calculated stearic acid area per molecule, nm^2	Variation range of stearic acid area per molecule, nm^2	Calculated stearic acid area per molecule, nm^2	Variation range of stearic acid area per molecule, nm^2
0.205	0.209	0.204–0.215	0.202	0.200–0.204
0.225	0.231		0.211	
0.230	0.233	0.226–0.241	0.213	0.202–0.222
0.250	0.263	0.258–0.271	0.216	0.209–0.223
0.273	0.274		0.226	
0.280	0.300	0.263–0.420	0.234	0.219–0.250
0.305	0.294		0.244	
0.320	0.402	0.321–0.565	0.371	0.297–0.666
0.348	0.385		0.611	
0.410	0.933		0.404	
0.444	6.035	0.000–2.342	0.808	0.637–1.587

based on our previous research.[50,52,54] The area per molecule value is related to the adsorption density as follows:

$$\text{Area per molecule} = \frac{1}{\Gamma \cdot N_A}, \tag{12}$$

where N_A is the Avogadro's number (6.023×10^{23}).

The area per molecule values calculated by the ERS adsorption density equation [Eq. (11)] are the average values of over ten individual measurements for both stearic acid films with and without calcium ions in the subphase. Without calcium ions in the subphase, the experimental Langmuir–Blodgett area per molecule values are in very good agreement with those values calculated using Eq. (11) for small areas. These results support the ERS adsorption density equation (11).

It is very interesting to compare experimental Langmuir–Blodgett area per molecule values with those values calculated using Eq. (11) with calcium ions in the subphase. When the experimental Langmuir–Blodgett area per molecule value is smaller than 0.28 nm^2/molecule but bigger than the taking off point for the condensed phase of the stearic acid isotherm 0.22 nm^2/molecule, the area per molecule values calculated from Eq. (11) are almost the same and much smaller than the experimental area per molecule value. These results suggest that the stearic acid molecules are oriented almost perpendicular to the water surface in distinct islands once they are formed even at zero pressure. The cartoons shown in Figs. 8 and 9 are intended to illustrate this observation further. From the above calculation, it is evident that in the case of calcium ion in the subphase the area per molecule reading from the isotherm and Table I column 1 is not able to represent the real molecule packing density and consequently the molecule phases. For example, when the apparent area per molecule reading from the isotherm is 0.28 nm^2 molecule^{-1}—adsorption density 5.93×10^{-6} mol/m^2, the measured area per molecule value from ERS equation is 0.234 nm^2 molecule^{-1}—adsorption density 7.10×10^{-6} mol/m^2. The apparent adsorption density from the isotherm is about 20% smaller than the measured adsorption density from ERS equation.

From these calculations and the isotherms discussed above, it is evident that the calculation of adsorption density using FTIR/ERS spectra can reveal the film phase at the air–water interface. However, only from the isotherm, the phase characteristics of the film cannot be directly determined. When the area per molecule values in the isotherm are greater than 0.22 nm^2, the molecule adsorption density can not be properly calculated from the isotherm in the case of calcium ions in the subphase. The phase characteristics of stearic acid film can also be derived from the shifting of CH

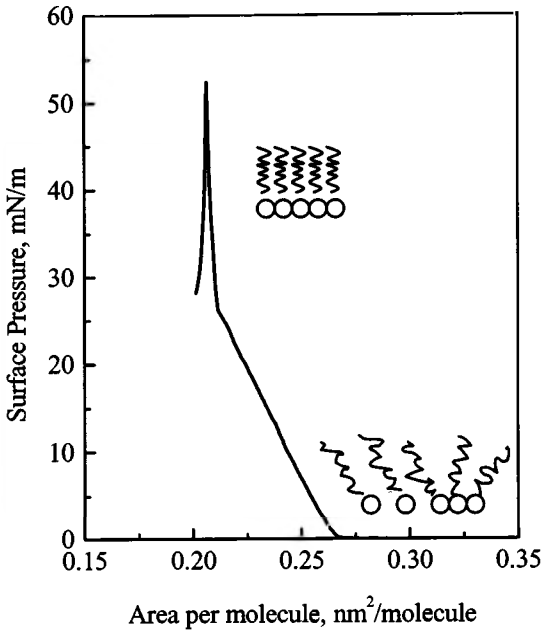

FIG. 8. Molecule orientation of stearic acid Langmuir–Blodgett films at air–water interface without calcium ions in the subphase.

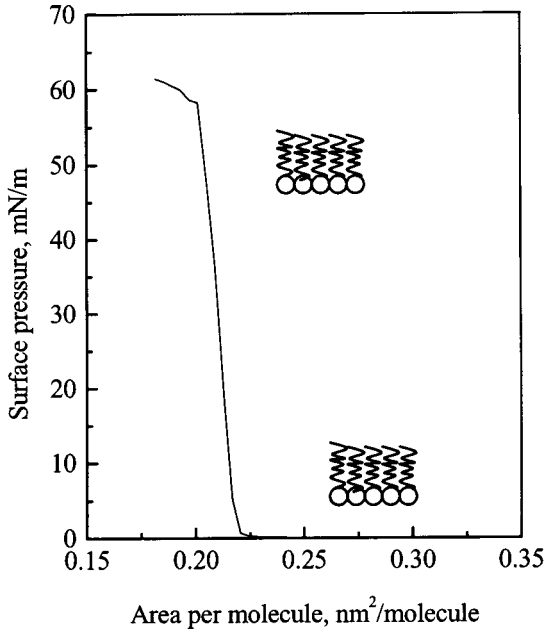

FIG. 9. Molecule orientation of stearic acid Langmuir–Blodgett films at air–water interface with calcium ions in the subphase.

peaks as stated above. However, only qualitative information can be obtained from the peak position analysis. First time in this research the real area per molecule values (or adsorption densities) of stearic acid Langmuir–Blodgett film were able to obtain from FTIR/ERS spectra.

E. Adsorption density of stearic acid at fluorite surface

Although the transferred film properties can be derived from the transfer ratio, the film may experience relaxation during and after transfer. The substrate may have some effects on the transferred film properties. It is thus necessary to directly probe the transferred film at the solid state substrate. The adsorption densities of stearic acid at fluorite surface calculated from the π-A isotherm and FTIR/ERS adsorption density equation were shown in Table II. The refractive index n_3 of fluorite used in the adsorption density calculation is 1.432.[31] The adsorption density values determined from FTIR/ERS spectra are again in good agreement with those calculated from the surface pressure-area isotherms. The difference between the adsorption densities calculated from isotherms and ERS equation may be explained as the film relaxation and substrate effects as stated above. Based on the adsorption density data above, it is believed that the adsorption density of stearic acid LB films with surface pressure less than 25 mN/m are on the order of from 6.5 to 7.5 μM/m^2. This result is also in good agreement with previous values reported in the literature.[54]

V. CONCLUSIONS

By comparison of calculated area per molecule values (nm^2/molecule) from the FTIR/ERS spectra with those obtained from the Langmuir–Blodgett area measurements, it is clear that the FTIR/ERS adsorption density equation is valid and can be used for quantitative analysis of surfactant Langmuir–Blodgett monolayers at the air–water interface and fluorite surface. The measurements need to be done with an appropriate experimental setup, sample preparation procedure, and proper signal detection. It is expected that this procedure for quantitative analysis of adsorbed surfactants will be useful in the biophysical, mineral processing, and the electronic and optical material fields.

As discussed in Sec. III, the adsorption density equation was derived based on an incident angle below 20° and no reflection from phase 3. Also it is necessary to know the angle ϕ in Eq. (11). This angle ϕ of the transition dipole moment with the surface normal must be measured *a priori* using appropriate spectroscopic techniques such as linear dichroism theory. Of course, for random surfactant organization (isotropic films), ϕ=45°. Since $1/\sin^2 75° = 1.0717$, for ϕ values from 90° to 75°, the adsorption density calculation is not very sensitive to the angle ϕ. For Langmuir–Blodgett films, a good guess of angle ϕ can be made. Under some circumstances the interface roughness between phases 2 and 3 may need to be taken into consideration.

Future research will consider other solid surfaces to further confirm the validity of the FTIR/ERS adsorption density equation. Also it is expected that the adsorption density of self-assembled films will be examined by the FTIR/ERS technique. Characterization of surfactant adsorption density on surfaces can help to explain the modification of surface properties. As long as the molecular absorptivity can be mea-

TABLE II. Adsorption densities calculated from ERS equation and isotherm for stearic acid at fluorite surface.

Transferred layer(s) without calcium ions in water	Area per molecule at transfer nm^2/molecule	Average density of every layer calculated from transfer isotherm (mol/m^2)	Average density of every layer calculated from FTIR/ERS spectra (mol/m^2)
1	0.208	7.98E-06	7.25E-06
1	0.223	7.45E-06	6.82E-06
1	0.225	7.38E-06	6.83E-06
1	0.231	7.19E-06	6.35E-06
1	0.241	6.89E-06	6.36E-06
With calcium ions in water			
1	0.203	8.18E-06	7.32E-06
3	0.209	7.94E-06	7.79E-06

sured or is known, Eq. (11) can be applied to other systems such as air–organic film/low absorbing dielectric substrate.

ACKNOWLEDGMENT

This research was supported by the DOE Office of Basic Sciences Grant No. DE-FG-03-93-ER14315.

[1] G. Roberts, *Langmuir–Blodgett Films* (Plenum, New York, 1990).
[2] M.-J. Hwang and K. Kim, Langmuir **15**, 3563 (1999).
[3] M. Liu, A. Kira, and H. Nakahara, J. Phys. Chem. **100**, 20138 (1996).
[4] M. Liu, G. Xu, Y. Liu, and Q. Chen, Langmuir **17**, 427 (2001).
[5] T. Kajiyama, L. Zhang, M. Uchida, Y. Oishi, and A. Takahara, Langmuir **9**, 760 (1993).
[6] A. Gericke and H. Huhnerfuss, Thin Solid Films **245**, 74 (1994).
[7] J. Simon-Kutscher, A. Gericke, and H. Huhnerfuss, Langmuir **12**, 1027 (1996).
[8] M. Yazdanian, H. Yu, and G. Zografi, Langmuir **8**, 630 (1992).
[9] L. F. Chi, R. R. Johnston, and H. Ringsdorf, Langmuir **7**, 2323 (1991).
[10] J. A. Zasadzinski, R. Viswanathan, L. Madsen, J. Garnaes, and D. K. Schwartz, Science **263**, 1726 (1994).
[11] M. C. Shih, T. M. Bohanon, J. M. Mikrut, P. Zshack, and P. Dutta, J. Chem. Phys. **96**, 1556 (1992).
[12] K. Kobayashi, K. Takaoka, S. Ochiai, Y. Taru, and M. Takasago, Thin Solid Films **210**, 559 (1992).
[13] M. Overs, F. Hoffmann, H. J. Schafer, and H. Huhnerfuss, Langmuir **16**, 6995 (2000).
[14] F. Hoffmann, H. Huhnerfuss, and K. J. Stine, Langmuir **14**, 4525 (1998).
[15] H. Huhnerfuss, V. Neumann, and K. J. Stine, Langmuir **12**, 2561 (1996).
[16] E. Pezron, R. M. Claesson, J. M. Berg, and D. Vollhard, J. Colloid Interface Sci. **138**, 245 (1990).
[17] L. F. Chi, M. Anders, H. Fuchs, R. R. Johnston, and H. Ringsdorf, Science **259**, 213 (1993).
[18] M. Yazdanian, H. Yu, and G. Zografi, Langmuir **8**, 630 (1992).
[19] J. T. Buoutempo and S. A. Rice, J. Chem. Phys. **98**, 5825 (1993).
[20] J. T. Buoutempo and S. A. Rice, J. Chem. Phys. **99**, 7030 (1993).
[21] R. A. Dluhy and D. G. Cornell, J. Phys. Chem. **89**, 3195 (1985).
[22] R. A. Dluhy, J. Phys. Chem. **90**, 1373 (1986).
[23] R. A. Dluhy, S. M. Stephens, S. Widayati, and A. D. Williams, Spectrochim. Acta, Part A **51**, 1413 (1995).
[24] D. L. Elmore and R. A. Dluhy, Colloids Surf. **171**, 225 (2000).
[25] D. L. Elmore and R. A. Dluhy, Appl. Spectrosc. **54**, 956 (2000).
[26] D. L. Elmore and R. A. Dluhy, J. Phys. Chem. B **105**, 11377 (2001).
[27] D. L. Elmore, S. Shanmukh, and R. A. Dluhy, J. Phys. Chem. A **106**, 3420 (2002).
[28] R. A. Dluhy, Ping Zhao, K. Faucher, and J. M. Brockman, Thin Solid Films **327–329**, 308 (1998).
[29] R. A. Dluhy and S. Stephens, Thin Solid Films **284–285**, 381 (1996).
[30] T. Hasegawa, J. Nishijo, Y. Kobayashi, and J. Umemura, Bull. Chem. Soc. Jpn. **70**, 525 (1997).
[31] J. A. Mielcazrske and E. Mielcazrske, J. Phys. Chem. **99**, 3206 (1995).
[32] J. A. Mielczarski, E. Mielczarski, and J. M. Cases, Langmuir **15**, 500 (1999).
[33] H. Hoffmann, U. Mayer, and A. Krischanitz, Langmuir **11**, 13.4 (1995).
[34] Y.-S. Yen and J. S. Wong, J. Phys. Chem. **93**, 7208 (1989).
[35] J. A. Mielcarski and R. H. Yoon, J. Phys. Chem. **93**, 2034 (1989).
[36] W. N. Hansen, *Advances in Electrochemistry and Electrochemical Engineering* (Wiley Interscience, New York, 1973), Vol. 9, Chap. 1.
[37] J. D. E. McIntyre, *Advances in Electrochemistry and Electrochemical Engineering* (Wiley Interscience, New York, 1973), Vol. 9, Chap. 2.
[38] W. N. Hansen, J. Opt. Soc. Am. **58**, 380 (1968).
[39] W. N. Hansen, Symp. Faraday Soc. **4**, 27 (1970).
[40] T. Iwata, J. Koshoubu, C. Jin, and Y. Okubo, Appl. Spectrosc. **51**, 1269 (1997).
[41] J. A. Mielczarski, J. Phys. Chem. **97**, 2649 (1993).
[42] M. D. Porter, Anal. Chem. **60**, 1143A (1988).
[43] H. Hoffmann, U. Mayer, and A. Krischantitz, Langmuir **11**, 1304 (1995).
[44] H. Brunner, U. Mayer, and H. Hoffmann, Appl. Spectrosc. **51**, 209 (1997).
[45] T. Hasegawa, J. Umemura, and T. Takenaka, J. Phys. Chem. **97**, 9009 (1993).
[46] T. Hasegawa, Y. Kobayashi, J. Nishijo, and J. Umemura, Vib. Spectrosc. **19**, 199 (1999).
[47] K. Fa, Ph.D. thesis, University of Utah.
[48] K. Fa, T. Jiang, J. Nalaskowski, and J. D. Miller (unpublished). The theoretically calculated spectra of stearic acid LB film at air–water interface were compared with the experimentally collected spectra. It was found that in the CH vibrational region, the calculated spectra were very similar to the spectra collected at the air–water interface. The influence of k values of water is negligible.
[49] W.-H. Jang and J. D. Miller, J. Phys. Chem. **99**, 10272 (1995).
[50] S. Frey and L. Tamm, Biophys. J. **60**, 922 (1991).
[51] T. Hasegawa, S. Takeda, A. Kawaguchi, and J. Umemura, Langmuir **11**, 1236 (1995).
[52] R. P. Sperline, Y. Song, and H. Freiser, Langmuir **13**, 3727 (1997).
[53] H. Sakai and J. Umemura, Bull. Chem. Soc. Jpn. **70**, 1027 (1997).
[54] W. H. Jang and J. D. Miller, Langmuir **9**, 3159 (1993).
[55] E. B. John and M. K. Ahmed, J. Phys. Chem. **93**, 2210 (1989).